

## Nucleic Acid Computation

International Edition: DOI: 10.1002/anie.201603265  
German Edition: DOI: 10.1002/ange.201603265

## Towards a DNA Nanoprocessor: Reusable Tile-Integrated DNA Circuits

Yulia V. Gerasimova and Dmitry M. Kolpashchikov\*

**Abstract:** Modern electronic microprocessors use semiconductor logic gates organized on a silicon chip to enable efficient inter-gate communication. Here, arrays of communicating DNA logic gates integrated on a single DNA tile were designed and used to process nucleic acid inputs in a reusable format. Our results lay the foundation for the development of a DNA nanoprocessor, a small and biocompatible device capable of performing complex analyses of DNA and RNA inputs.

Logic gates are devices that recognize one or more inputs, process them according to a certain input–output signal correlation pattern, and produce a single binary output, which can be either high or low: a digital 1 or 0, respectively.<sup>[1]</sup> For example, a two-input Boolean logic gate with the AND function produces a high output (digital 1) only when both inputs are present, with the output remaining low (digital 0) for all other input combinations (Figure 1A, truth table). Current microprocessor systems are based on logic gates that employ electronic input and output signals and power supplies.<sup>[1]</sup> However, the nature of the inputs and outputs is not limited to electric signals. For example, some early computers used mechanical movements of their components as input/output signals.<sup>[2]</sup>

It has been proposed that significant miniaturization of computational elements could be achieved if they were made of individual molecules,<sup>[3]</sup> and such molecular computers are “the inevitable wave of the future”.<sup>[3b]</sup> Smaller devices would reduce energy and material consumption.<sup>[3]</sup> Since the first publication by de Silva et al.,<sup>[4]</sup> a great variety of molecular logic gates have been designed toward this goal.<sup>[5]</sup> DNA has been considered a promising molecule for constructing molecular devices including logic gates due to the highly selective and predictable interactions between the Watson–Crick base pairs, A–T and G–C.<sup>[6]</sup> A computer made of DNA could be used to control the action of biocompatible devices for the diagnosis and treatment of diseases such as cancer, bacterial and viral infections, and genetic disorders. One example of DNA-based logic circuits is an array of deoxyribozyme gates, which can play tic-tac-toe with humans.<sup>[7]</sup> Another remarkable example are seesaw gates,<sup>[8]</sup> which can be arranged in a DNA strand displacement cascade that mimics a neural network.<sup>[9]</sup> However, the majority of DNA-

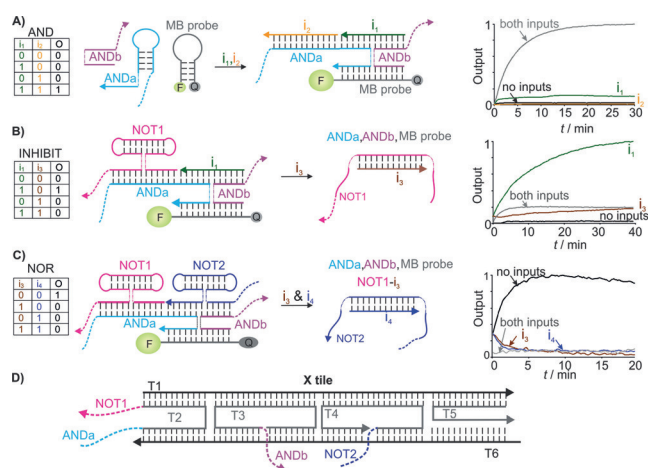


**Figure 1.** Design of tile-integrated DNA circuits. A) Two-input 4J AND gate. The gate consisted of ANDa, ANDb, and an MB probe. The ANDa and ANDb strands contained the sequences complementary to the “hook” sequences (dashed lines) of the X tile (D), while the input strands and the MB probe operated as free (tile-unbound) molecules. The five-stranded 4J association was formed in the presence of both inputs  $i_1$  and  $i_2$ . B) The two-input 4J INHIBIT1 gate consisted of the same components as the 4J AND gate plus the NOT1 strand, which itself operated as an inverter (NOT gate). The output fragments of the NOT1 strand were complementary to strand ANDa and opened its folded structure similarly to input  $i_2$ . In the presence of input  $i_1$ , the 4J complex was formed, which generated a high output signal. The addition of input  $i_3$ , which was complementary to the middle fragment of the NOT1 gate, removed the NOT1 strand from the 4J complex, thus triggering its dissociation and decreasing the fluorescence signal. C) Two-input 4J NOR gate. In the absence of inputs, the terminal output fragments of both NOT gates were bound to the input-recognition fragments of the AND gate, which enabled the formation of the high-signal 4J NOR association. The addition of the  $i_3$  and/or  $i_4$  inputs, which were complementary to NOT1 and NOT2, respectively, resulted in dissociation of the 4J NOR complex similarly to the 4J INHIBIT high-signal complex, thus switching off the gate. For (A), (B), and (C), dashed lines represent fragments complementary to the “hook” sequences of the DNA X tile; the output is presented as normalized fluorescence signal. D) The DNA X tile. The “hook” sequences (dashed fragments) are shown in the same color as the complementary fragments of the gate strands. More details are shown in the Supporting Information, Figure S1.

based logic circuits use molecules that diffuse freely in solution, which slows the response and requires careful design of each new DNA construct to avoid gate miscommunication. The implementation of concerted arrays of communicating molecules remains challenging.<sup>[10]</sup> Here, inspired by the strategy used for manufacturing conventional electronic processors, we positioned DNA logic gates in a precise order on a two-dimensional (2D) platform.

[\*] Dr. Y. V. Gerasimova, Dr. D. M. Kolpashchikov  
Chemistry Department, University of Central Florida  
Orlando, FL 32816 (USA)  
E-mail: Dmitry.Kolpashchikov@ucf.edu

Supporting information for this article can be found under:  
<http://dx.doi.org/10.1002/anie.201603265>.

We constructed an AND gate and combined it with NOT gates to obtain integrated circuits that process oligonucleotide inputs according to INHIBIT and NOR logic (Figure 1). Each logic gate consisted of several DNA strands, which hybridized with oligonucleotide inputs and formed associations stabilized by the DNA three-way junction (4J) structure<sup>[11]</sup> when the output was high. The 4J structures dissociated into separate strands when the output was low. We therefore named these logic DNA gates “4J gates”. The 4J structures were conveniently detected using a molecular beacon (MB) probe, a fluorophore- and quencher-conjugated stem-loop folded DNA strand<sup>[12]</sup> (Figure 1A). The folded MB structure kept the fluorophore close to the quencher, thus producing low fluorescence in the case of a low output. High fluorescence was produced upon association of the MB probe with the 4J structures, as this association caused the MB probe to acquire its elongated conformation.<sup>[12c,d]</sup> The 4J gate design preserved input/output homogeneity, which is important for the integration of logic gates into circuits. Indeed, the undoubted success of modern computers is in part because the electronic output of one gate can be recognized as an input of the downstream gate. Likewise, an output of one 4J gate, which is a nucleotide sequence made of two separate fragments, can be recognized as an input by the next gate. Although the design principles for AND and INHIBIT gates in solution were reported previously by us,<sup>[13]</sup> significant structural adjustments were introduced in this study to enable the proper operation of the 4J gates on a 2D scaffold (see the Supporting Information, Figure S1 for more details). The design of the NOR gate is reported here for the first time.

As a 2D platform, we used a DNA crossover (X) tile,<sup>[14]</sup> a well-characterized building block extensively used in DNA nanotechnology<sup>[15]</sup> for constructing nanoscale DNA structures. The X tile was made of six DNA strands assembled in a complex, as shown in Figure 1D. Four tile-forming strands were equipped with the “hook” sequences for the attachment of DNA logic gates (dashed lines in Figure 1D). According to our design, all four hook fragments should face the same side of the tile. The overall idea of the tile-integrated DNA circuits was that logic gate strands form 4J complexes when an input combination corresponds to a high output, thus passing the signal across the entire surface of the tile. These complexes dissociate into separate strands when the output is low.

Tile strands were annealed with the 4J gate strands to form the tile-associated DNA logic gates. Analysis of the tile and gate-tile complexes using agarose gel electrophoresis revealed the formation of homogeneous associations with the expected migration in the gel (Supporting Information, Figure S2). No noticeable inter-tile associations were detected for all input combinations (Supporting Information, Figure S2A and C), which indicates minimal or no inter-tile interactions for this design. Isolation of the tile bands followed by PAGE analysis demonstrated the presence of all expected strands in the corresponding DNA associations (Supporting Information, Figure S2B). As expected, the AND gate produced high fluorescent output in the presence of both inputs (Figure 1A). The digital output 1 could be distinguished from output 0 seconds after the input addition. The fluorescent response reached a plateau in approximately

15 min, a performance similar to that of the hybridization of a MB probe to a complementary target in solution.<sup>[16]</sup> Therefore, it can be assumed that the rate of high-fluorescence complex formation shown in Figure 1 is limited by the hybridization of the MB probe from solution and does not reflect the rate of tile-bound gate-to-gate communication. A two-input INHIBIT gate produced a high output in the presence of only one particular input ( $i_1$ ), while the fluorescent output remained low for all other input combinations, according to the truth table (Figure 1B). An alternative 4J INHIBIT gate (INHIBIT 2) operated in a similar mode (Supporting Information, Figure S3C), with input  $i_1$  and the NOT1 strand replaced by NOT2 and  $i_2$ , respectively (Supporting Information, Figure S1G).

Modern digital electronics takes advantage of the functionally complete operator, a set of logic gates that can be combined to generate every possible logical function. One such operator is the NOR logic, which produces a high output only when both inputs are absent (Figure 1C). We therefore designed a NOR gate function by integrating two NOT and one AND gates, as shown in Figure 1C. In this design, the output fragments of the two NOT gates were recognized as inputs by the AND gate, which is a simple example of integrated DNA circuits. The digital response was as expected, based on fluorescence monitoring (Figure 1C, right). None of the DNA 4J gates used in this study produced a proper digital response when detached from the tile (Supporting Information, Figure S3). This result proved that the attachment of the gate strands to the X tile is essential for the circuit operation. Two major factors contribute to the improved communication of the interrogated gates: the increased local concentration of the gate strands attached to the tile; and the prevention of the incorrect strand interactions due to their positioning on the 2D support.<sup>[17]</sup> Our data (Supporting Information, Figures S3, S4) indicate that both factors are important. We, therefore, conclude that the design of the tile and the linkers enabled proper orientation and provided sufficient flexibility for the formation of the 4J complexes, as shown in Figure 1.

For practical applications of computational circuits it is important to enable the resetting and, therefore, reuse of the computational circuits.<sup>[18]</sup> For this purpose, we added RNase H as a buffer component. RNase H is an enzyme that catalyzes the hydrolysis of RNA in RNA–DNA duplexes<sup>[19]</sup> and was used previously for building DNA oscillating systems.<sup>[20]</sup> We replaced DNA inputs  $i_1$  and  $i_3$  with their ribo-analogues (ribo- $i_1$  and ribo- $i_3$ ). The fluorescence of the samples was monitored continuously in a time-drive mode (Figure 2). For the 4J INHIBIT gate, the signal increased within the first 5 min upon addition of ribo- $i_1$ , which reflected the formation of the 4J association, until the competing hydrolysis of the input strand began to predominate, which gradually decreased the fluorescence (Figure 2A). When the signal decreased, a second portion of the ribo- $i_1$  was added (indicated by an arrow at 16 min in Figure 2A), which led to the second increase in the fluorescent output. This oscillating behavior of the DNA logic gate was demonstrated for at least three consecutive cycles. Similar multiple operations were demonstrated for the NOR gate, in which the addition of one

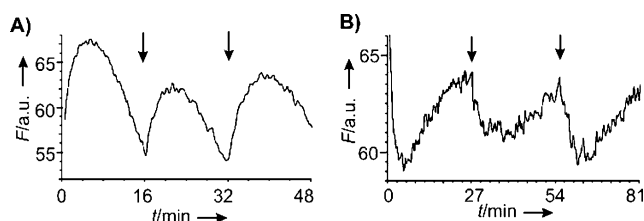


**Figure 2.** Resetting of 4J gates in response to ribo-inputs in the presence of RNase H. A) Fluorescent response of 4J-INHIBIT1 as a function of time. The arrows indicate time points when a new portion of ribo- $i_1$  was added (every 16 min). B) Fluorescent response of 4J-NOR as a function of time. The arrows indicate time points of ribo- $i_3$  addition (every 27 min).

input ( $i_3$ ) reduced the fluorescent output as expected (Figure 2B). Unlike for the INHIBIT gate, degradation of ribo- $i_3$  by RNase H could not fully restore the ON state of the NOR gate (the maximum fluorescent signal for the resetting mode was lower than the ON state fluorescence for the one-time mode of the gate operation). This may be explained by the accumulation of short degradation products of ribo- $i_3$  by RNase H,<sup>[18]</sup> which block at least one of the signal-transmitting arms of the NOT gate, thus inhibiting the communication between the NOT and AND gates.

A number of research groups have reported on the design of molecular ensembles that perform logic operations.<sup>[6–10]</sup> Even though molecular devices that use non-Boolean logic operations have been considered for the control and analysis of biological systems,<sup>[21]</sup> here we used Boolean DNA logic gates to take a step on a path that mimics the development of modern electronic computers. We report a proof-of-principle technology for the production of DNA logic circuits localized on a 2D platform formed by a crossover DNA tile. We integrated three DNA logic gates (two NOT and one AND) in a circuit. We demonstrated that gate response and enzyme-dependent resetting can be achieved in minutes, which is presumably limited by binding of MB probe reporter from solution. However, the rate of tile-associated gate-to-gate communication remains to be investigated in future studies. Some important features of the design are as follows: 1) The 4J DNA logic gates recognize DNA or RNA inputs and produce output as DNA fragments, and this input–output homogeneity opens the possibility of building complex integrated circuits in a modular fashion; 2) the 4J-forming logic operators are positioned on a 4J-forming DNA tile; this structural similarity simplifies the localization of the logic gate strands on the X tile for proper communication; 3) the gate strands reversibly associate when the output is high, thus propagating the signal through the surface of the tile; and 4) the 4J tile enables the attachment of multiple strands, as well as potential association of multiple tiles<sup>[14c]</sup> into larger integrated circuits.

In conclusion, we proposed a new design principle for DNA logic gates integrated in a DNA circuit on a 2D platform. We manufactured approximately  $10^{14}$  DNA circuits in 1 mL of the hybridization mixture in 16 h with a hands-on time of 5 min using only two micropipettes and a hot plate. The estimated cost of each particle of 4J integrated DNA

circuits was only  $\$10^{-11}$ , which can be readily reduced by a factor of at least  $10^3$  if scaled up. We achieved the expected digital responses and circuit resetting within minutes. The next step would be the extension of this technology to build more elaborate networks of communicating logic gates and the assessment of their computational capabilities.

## Experimental Section

**Preparation of DNA X tile:** Oligonucleotide strands of the tile and desired combination of logic gate strands (200 nM each) were mixed in  $2 \times$  working buffer containing 100 mM Tris-HCl (pH 7.0) and 100 mM  $MgCl_2$  to make  $2 \times$  stock solutions of the tile-associated DNA logic gates. The mixtures were heated at  $95^\circ\text{C}$  in a 2 L water bath and gradually cooled to room temperature over 20 h. The formation of DNA associations was checked using 2% agarose gel electrophoresis.

**Fluorescence assay:** Samples containing MB reporter (20 nM) and 100 nM tile-associated DNA logic gates in  $1 \times$  working buffer were incubated in the absence of inputs or in the presence of different combinations of input oligonucleotides (1000 nM) at room temperature ( $20\text{--}22^\circ\text{C}$ ). Fluorescence of the samples upon excitation at 485 nm was monitored at 517 nm using a PerkinElmer LS 55 fluorescence spectrometer (Waltham, MA, USA) in the time-drive mode or in the spectrum mode after a specified incubation period.

**Resetting of the tile-associated gate:** A sample containing  $0.1 \mu\text{L}^{-1}$  RNase H, MB reporter (20 nM) and a tile-associated INHIBIT or NOR gate (100 nM) in  $1 \times$  working buffer was incubated at room temperature for 10 min to ensure the formation of the DNA association with the MB reporter in the absence of inputs. Then, an input oligonucleotide (1000 nM) was added to the sample, and the fluorescence signal at 517 nm upon excitation at 485 nm was continuously monitored in a time-drive mode. At specified time points (every 16 min for INHIBIT gate, every 27 min for NOR gate), a new portion of the input was added to the sample to start a new cycle of logic gate operation. At least three cycles of operation were demonstrated for both INHIBIT and NOR 4J-logic gates assembled on a DNA X tile.

## Acknowledgements

Financial support from the NSF CCF 1423219 is gratefully acknowledged.

**Keywords:** crossover DNA tiles · DNA logic gates · molecular beacons · molecular computation · NOR gates

**How to cite:** *Angew. Chem. Int. Ed.* **2016**, 55, 10244–10247  
*Angew. Chem.* **2016**, 128, 10400–10403

- [1] A. P. Malvino, J. A. Brown, *Digital computer electronics*, 3rd ed., Glencoe, Lake Forest, **1993**.
- [2] A. G. Bromley, *IEEE Ann. Hist. Comput.* **1983**, 4, 197–217.
- [3] a) R. P. Feynman, *Eng. Sci.* **1950**, 23, 22; b) P. Ball, *Nature* **2000**, 406, 118.
- [4] A. P. De Silva, H. Q. N. Gunaratne, C. P. McCoy, *Nature* **1993**, 364, 42.
- [5] a) A. P. De Silva, Y. Leydet, C. Lincheneau, N. D. McClenaghan, *J. Phys.* **2006**, 18, S1847; b) K. Szaciłowski, *Chem. Rev.* **2008**, 108, 3481, and references therein; c) Y. Benenson, *Nat. Rev. Genet.* **2012**, 13, 455–468; d) J. Andréasson, U. Pischel, *Chem. Soc. Rev.* **2015**, 44, 1053, and references therein; e) M. N. Stojanovic, D. Stefanovic, S. Rudchenko, *Acc. Chem. Res.* **2014**, 47, 1845; f) R. Orbach, B. Willner, I. Willner, *Chem. Commun.* **2015**, 51, 4144.



- [6] a) M. N. Stojanovic, T. E. Mitchell, D. Stefanovic, *J. Am. Chem. Soc.* **2002**, *124*, 3555; b) A. Okamoto, K. Tanaka, I. Saito, *J. Am. Chem. Soc.* **2004**, *126*, 9458; c) B. M. Frezza, S. L. Cockcroft, M. R. Ghadiri, *J. Am. Chem. Soc.* **2007**, *129*, 14875; d) Y. Krishnan, F. C. Simmel, *Angew. Chem. Int. Ed.* **2011**, *50*, 3124–3156; *Angew. Chem.* **2011**, *123*, 3180–3215; e) K. S. Park, M. W. Seo, C. Jung, J. Y. Lee, H. G. Park, *Small* **2012**, *8*, 2203; f) A. Prokup, J. Hemphill, A. Deiters, *J. Am. Chem. Soc.* **2012**, *134*, 3810; g) A. Padirac, T. Fujii, Y. Rondelez, *Curr. Opin. Biotechnol.* **2013**, *24*, 575; h) F. Wang, C.-H. Lu, I. Willner, *Chem. Rev.* **2014**, *114*, 2881; i) K. Furukawa, N. Minakawa, *Org. Biomol. Chem.* **2014**, *12*, 3344; j) D. Han, H. Kang, T. Zhang, C. Wu, C. Zhou, M. You, Z. Chen, X. Zhang, W. Tan, *Chem. Eur. J.* **2014**, *20*, 5866; k) C. W. Brown III, M. R. Lakin, E. K. Horwitz, M. L. Fanning, H. E. West, D. Stefanovic, S. W. Graves, *Angew. Chem. Int. Ed.* **2014**, *53*, 7183; *Angew. Chem.* **2014**, *126*, 7311; l) Y. V. Gerasimova, D. M. Kolpashchikov, *Chem. Commun.* **2015**, *51*, 870; m) A. Prokup, J. Hemphill, Q. Liu, A. Deiters, *ACS Synth. Biol.* **2015**, *4*, 1064; n) S. Mailloux, Y. V. Gerasimova, N. Guz, D. M. Kolpashchikov, E. Katz, *Angew. Chem. Int. Ed.* **2015**, *54*, 6562; *Angew. Chem.* **2015**, *127*, 6662; o) S. Bi, J. Ye, Y. Dong, H. Li, W. Cao, *Chem. Commun.* **2016**, *52*, 402; p) R. Orbach, F. Wang, O. Lioubashevski, R. D. Levine, F. Remacle, I. Willner, *Chem. Sci.* **2014**, *5*, 3381; q) L. Freage, A. Trifonov, R. Tel-Vered, E. Golub, F. Wang, J. S. McCaskill, I. Willner, *Chem. Sci.* **2015**, *6*, 3544.
- [7] M. N. Stojanovic, D. Stefanovic, *Nat. Biotechnol.* **2003**, *21*, 1069.
- [8] G. Seelig, D. Soloveichik, D. Y. Zhang, E. Winfree, *Science* **2006**, *314*, 1585.
- [9] L. Qian, E. Winfree, J. Bruck, *Nature* **2011**, *475*, 368.
- [10] A. P. De Silva, S. Uchiyama, *Nat. Nanotechnol.* **2007**, *2*, 399.
- [11] D. M. Lilley, *Q. Rev. Biophys.* **2000**, *33*, 109.
- [12] a) S. Tyagi, F. R. Kramer, *Nat. Biotechnol.* **1996**, *14*, 303; b) D. M. Kolpashchikov, *Scientifica* **2012**, 928783, and references therein; c) D. M. Kolpashchikov, *J. Am. Chem. Soc.* **2006**, *128*, 10625; d) Y. V. Gerasimova, A. Hayson, J. Ballantyne, D. M. Kolpashchikov, *ChemBioChem* **2010**, *11*, 1762.
- [13] a) A. Lake, S. Shang, D. M. Kolpashchikov, *Angew. Chem. Int. Ed.* **2010**, *49*, 4459; *Angew. Chem.* **2010**, *122*, 4561; b) Y. V. Gerasimova, D. M. Kolpashchikov, *Chem. Asian J.* **2012**, *7*, 534.
- [14] a) T.-J. Fu, N. C. Seeman, *Biochemistry* **1993**, *32*, 3211; b) A. V. Garibotti, S. M. Knudsen, A. D. Ellington, N. C. Seeman, *Nano Lett.* **2006**, *6*, 1505; c) B. Kim, S. Jo, J. Son, J. Kim, M. H. Kim, S. U. Hwang, S. R. Dugasani, B. D. Kim, W. K. Liu, M. K. Kim, S. H. Park, *Nanotechnology* **2014**, *25*, 105601.
- [15] a) N. C. Seeman, *Nature* **2003**, *421*, 427; b) J. Son, J. Lee, A. Tandon, B. Kim, S. Yoo, C. W. Lee, S. H. Park, *Nanoscale* **2015**, *7*, 6492.
- [16] Y. V. Gerasimova, D. M. Kolpashchikov, *Biosens. Bioelectron.* **2013**, *41*, 386.
- [17] a) R. A. Muscat, K. Strauss, L. Ceze, G. Seelig, *ACM SIGARCH Computer Architecture News* **2013**, *41*, 177; b) M. Teichmann, E. Kopperger, F. C. Simmel, *ACS Nano* **2014**, *8*, 8487; c) N. Dalchau, H. Chandran, N. Gopalakrishnan, A. Phillips, J. Reif, *ACS Synth. Biol.* **2015**, *4*, 898.
- [18] a) A. J. Genot, J. Bath, A. J. Turberfield, *J. Am. Chem. Soc.* **2011**, *133*, 20080–20083; b) M. Zhang, B. C. Ye, *Chem. Commun.* **2012**, *48*, 3647; c) M. R. O'Steen, E. M. Cornett, D. M. Kolpashchikov, *Chem. Commun.* **2015**, *51*, 1429; d) D. Y. Tam, Z. Dai, M. S. Chan, L. S. Liu, M. C. Cheung, F. Bolze, C. Tin, P. K. Lo, *Angew. Chem. Int. Ed.* **2016**, *55*, 164; *Angew. Chem.* **2016**, *128*, 172.
- [19] S. T. Croke, K. M. Lemonidis, L. Neilson, R. Griffey, E. A. Lesnik, B. P. Monia, *Biochem. J.* **1995**, *312*, 599.
- [20] a) J. Kim, E. Winfree, *Mol. Syst. Biol.* **2011**, *7*, 465; b) J. Kim, K. S. White, E. Winfree, *Mol. Syst. Biol.* **2006**, *2*, 68; c) M. Weitz, J. Kim, K. Kapsner, E. Winfree, E. Franco, F. C. Simmel, *Nat. Chem.* **2014**, *6*, 295.
- [21] a) Q. Chen, S. Y. Yoo, Y. H. Chung, J. Y. Lee, J. Min, J. W. Choi, *Bioelectrochemistry* **2016**, *111*, 1; b) P. Siuti, J. Yazbek, T. K. Lu, *Nat. Biotechnol.* **2013**, *31*, 448; c) B. S. Chen, C. Y. Hsu, J. J. Liou, *J. Biomed. Biotechnol.* **2011**, *2011*, 304236; d) V. Privman, G. Strack, D. Solenov, M. Pita, E. Katz, *J. Phys. Chem. B* **2008**, *112*, 11777–11784; e) N. Guz, T. A. Fedotova, B. E. Fratto, O. Schlesinger, L. Alfonta, D. M. Kolpashchikov, E. Katz, *Chem-PhysChem* **2016**, DOI: 10.1002/cphc.201600129.

Received: April 3, 2016

Revised: June 5, 2016

Published online: July 19, 2016